TA-Fe(III) complex coated PS nanospheres for non-iridescent structural coloration of cotton fabric

Xiaowei Zhu
Soochow University
Tianchen Wei
Soochow University
Yijiang Li
Soochow University
Yichen Li (ycli131@suda.edu.cn)
Soochow University
Tieling Xing
Soochow University
Matthew D. Shawkey
University of Ghent
Guoqiang Chen
Soochow University

Research Article

Keywords: Structural color, Tannic acid, Cotton fabric, Shell-core nanospheres, Non-iridescent, Amorphous colloidal arrays

Posted Date: August 4th, 2022

DOI: https://doi.org/10.21203/rs.3.rs-1905579/v1

Abstract

Photonic structures constructed from colloidal nanospheres present an attractive prospect for structural coloration in an ecological manner. However, the application of structural color in the field of textile coloration is usually blocked by their uncorrelated scattered light and feeble mechanical properties. Here, a non-iridescent structural color coating with high color saturation and mechanical stability is developed by assembling PS@TA-Fe(III) core-shell nanospheres. The rough surface and low surface charge are favorable for forming amorphous colloid arrays (ACAs) by restricting the crystalline alignment during the assembly process, resulting in non-iridescent structural colors. In addition, the as-prepared structurally colored cotton fabric possess high color saturation and mechanical stability thanks to the intense light absorption and interface adhesion of the TA-Fe(III) shell. The preparation approach of this structural color coating is facile, low-cost, and environment-friendly, showing promising applications in textile coloration and smart display.

Introduction

Structural coloration, which is a bio-inspired phenomenon that produces brilliant colors from the light-matter interaction between visible light and submicrometer dielectric structures. The well-orderly arranged photonic crystal structures(PCs) using colloidal nanoparticles as the building blocks is one of the most studied structural color materials recently, due to its saturated and bright colors (Chen et al. 2019). However, the ordered periodic structure of photonic crystals usually causes optical anisotropy resulting in an angle-dependent structural color, which will significantly restrict their application in some fields, such as displays and sensors (Shen et al. 2020). Compared with the high ordering of PCS, amorphous colloid arrays (ACAs) possess a short-range order but long-range disorder periodicity, which is a particular defect state structure (Ge et al. 2014). Due to the low lattice arrangement ordering of ACAs, natural light scatters multiple times when passing through the defects in the medium, forming an isotropic photon pseudo-bandgap with the action of interference (Ge et al. 2014; Takeoka 2012). The wavelength position and intensity of this photon pseudo-bandgap basically do not change with the angle of incident light (Iwata et al. 2017; Liu et al. 2018; Takeoka et al. 2013), causing isotropic coherent scattering, then producing non-iridescent structural colors (Liu et al. 2020; Okada et al. 2021; Shi et al. 2020; Yang et al. 2020).

The coherent scatting by the ACAs is usually diluted by the incoherently scattered light from the individual nanoparticles, resulting in a pale and faded color (Kohri et al. 2015; Li et al. 2019; Yuan et al. 2015). The incoherent light scatting can be eliminated by introducing black elements with broadband light absorption, such as carbon black (Li et al. 2021), graphene (Zhang et al. 2018), polypyrrole (Yang et al. 2016), and melanin (Kohri et al. 2020), into the photonic systems, resulting in an increase in brightness and saturation of the resultant structural colors. Polydopamine(PDA), inspired by mussels, is one of the most widely studied synthetic melanin and has attracted much attention due to its versatility and simplicity (Xiao et al. 2015, 2020). Moreover, similar to the adhesion mechanism of natural mussel protein, a large amount of catechol and amino groups on PDA can also facilitate it adheres to almost all substrate surfaces, regardless of its physical and chemical properties (Xiao et al. 2017). Accordingly, as a

black substance with excellent adhesion properties, PDA has been recognized as an ideal material to modify the surface of colloidal nanoparticles for constructing photonic nanostructures. Shi et al. coated poly(styrene-methyl methacrylate-acrylic acid) latex nanospheres with a thin PDA shell and assembled the as-prepared core-shell nanospheres on cotton fabric to obtain structurally colored fabric with high color saturation and excellent color fastness (Shi et al. 2019). Furthermore, Zhu et al. proposed a rapid strategy to prepare melanin-like nanoparticles by copper ion-promoted polymerization of DA to coat PS nanospheres for fascinating structural coloration (Zhu et al. 2021). Such melanin-like particles can not only be used as the building blocks of the photonic nanostructure but also as light-absorbing elements to enhance the saturation of the resultant structural colors (Kohri et al. 2020), which has become a research hotspot in the fields of structural coloration.

Although the incorporation of PDA into the PC system can significantly improve the structural stability and color saturation, the high cost of DA has been considered an obstacle to its industrial application. Due to the similarity in molecular structure with DA and DOPA, plant-derived polyphenols, which are the secondary metabolites of plants, also possess vigorous solid-liquid interfacial activity and can firmly adhere to various substrates through covalent and non-covalent interactions (Rahim et al. 2014). Sileika et al. have reported the spontaneous formation of thin polyphenol coatings on various chemically inert surfaces when exposed to polyphenol-rich beverages (Sileika et al. 2013). Consequently, it is of great significance to use the excellent properties of plant polyphenols to develop intriguing structural color materials. Tannic acid (TA), the third-largest plant component (tannin substance) in nature, belongs to the group of high molecular weight phenolic compounds and contains five digalloylester groups covalently attached to a central glucose core (Guo et al. 2014; Perron et al. 2009; Wang et al. 2020). Metal chelation is a salient feature of TA (like many other polyphenols), upon which it acts as a polydentate ligand for metal ion coordination.

Herein, inspired by the high catechol content of mussel adhesion proteins and the involvement of catechol in melanin biosynthesis, a cheap and environmentally friendly coating strategy was demonstrated to prepare PS@TA-Fe(III) core-shell nanospheres, which can create non-iridescent bright structural colors. Natural polyphenol-TA and Fe(III) were used as organic ligands and inorganic crosslinking agents. The metal-polyphenol network membrane was formed on the surface of PS nanospheres by utilizing the chelation of TA and Fe(III) and the adhesion of TA to the template at the moment of mixing. Notably, the preparation process is green, and environmentally friendly, and the wastewater generated during the preparation process can be directly discharged without pollution to the environment. Although the cotton fabric background was white, the structurally colored coating can exhibit excellent color saturation and did not change with the angle. The tests, including simulated washing tests, folding tests, and sandpaper abrasion, further demonstrated the high color fastness of the PS@TA-Fe(III) coating. This facile and novel strategy can fabricate bright and non-iridescent structural colored material, which can also be applied in the color display field and may boost the prospect of ACAs.

Materials And Methods

Materials

Cotton fabric (twill fabric, 103 g/m^2, warp density: 40 threads per cm; weft density: 22 threads per cm) was provided by Jiangsu Shazhou Printing and Dyeing group (China) and used after being washed with lye soap. Styrene (St, 99%), sodium dodecyl sulfate (SDS, 99%), and potassium persulfate (KPS, 99%) were purchased from Aladdin Co. Ltd. Ferric chloride anhydrous ($FeCl_3$) were supplied by Sinopharm Chemical Reagent Co., Ltd. Tannic acid (TA, AR) was obtained from Shanghai Lingfeng Chemical Reagent Co.; Ltd. All the chemicals were of analytical reagent grade and used without further purification.

Synthesis of monodisperse PS nanospheres

The monodisperse PS nanospheres were synthesized by an emulsion polymerization method. For a typical synthesis of PS nanospheres with an average size of 225 nm, 10 g St was added into a four-necked and round-bottomed flask of 250 mL volume, with 85 mL H_2O containing 0.06 g SDS, and stirred vigorously at 350 rpm for 10 min under nitrogen atmosphere. Subsequently, after the temperature was raised to 85°C, 5 mL of an aqueous solution containing 0.07 g KPS was added quickly into the flask to initiate the polymerization reaction of St. After 8 h of reaction, monodisperse PS nanospheres were obtained. Remarkably, the size of PS nanospheres could be easily manipulated by adjusting the amounts of SDS and KPS.

Synthesis of PS@TA-Fe(III) core-shell nanospheres

In a typical procedure, 1 mL PS dispersion (10 wt%) was dissolved in 50 mL deionized water and ultrasonically dispersed for 10 minutes to form a uniform colloidal dispersion. After that, the diluted PS dispersion was stirred magnetically at 60 ℃ for 1 min with a stirring speed of 1400 r/min. Subsequently, TA (0.06 mmol) and $FeCl_3$ (0.06 mmol) were added to the PS nanoparticles dispersion to react for 20 s. Then, the resultant PS@TA-Fe(III) nanoparticles with a TA-Fe(III) shell coated on a PS core were centrifuged and washed three times with DI water for purification. Finally, the PS@TA-Fe(III) nanospheres were redispersed in DI water to form a colloidal suspension with a concentration of 5 wt % for later usage.

Fabrication of non-iridescent structural colors on white cotton fabric

The PS@TA-Fe(III) nanospheres were used to fabricate ACAs on cotton fabric surface by gravity deposition self-assembly. Firstly, 5 mL of PS@TA-Fe(III) nanoparticles dispersion was dropped into a Petri dish (6 cm in diameter) with a piece of white cotton fabric. The sample was placed in an oven with a temperature of 60°C until the fabric was dried entirely, and then increased the temperature to 80°C for 2 hours to ensure the ACAs coating firmly adhered to the surface of the fabric substrate. As a reference, bare PS nanospheres were assembled on the surface of cotton fabric by the same method.

Characterization

The element content of the sample surface was analyzed by X-ray photoelectron spectroscopy (XPS, Thermo ESCALAB 250XI, USA) with Al Ka excitation radiation (1484.6 eV). The morphology of the ACAs

was observed by a field emission scanning electron microscopy (FESEM, Hitachi S-4800, Japan). The morphology of the nanospheres was obtained using transmission electron microscopy (TEM, HT7700, Japan). The total reflection spectrum was measured by an ARM-type micro-angle-resolving spectrometer (Shanghai Fuxiang Instrument Equipment Co., Ltd.). The color fastness and washing resistance of the structurally colored fabric were examined by a sandpaper abrasion test and simulated washing test, respectively (Meng et al. 2017; Zhou et al. 2016). The BOD_5 value of wastewater was measured according to the Water Quality Five-Day Biochemical Oxygen Demand (BOD_5) Determination of Dilution and Inoculation Method. The COD value of wastewater was measured according to Water Quality Chemical Oxygen Demand Determination Dichromate Method (HJ 828–2017). The chromaticity of wastewater was measured according to the international standard ISO 7887 − 1985 (Inspection and Determination of Color).

Results And Discussion

Formation mechanism of TA-Fe(III) shell

Typically, the two adjacent hydroxyl groups on catechol or galloyl groups of phenolic compounds can provide binding sites for metal ions to chelate (Ejima et al. 2013). Consequently, TA can form highly stable complexes with Fe(III), ranging from mono-type to tris-type complexes (Perron et al. 2009). When the pH of the reaction system is less than 2, TA and Fe(III) form colorless mono-complex; then, with the pH increases to between 3 to 6, TA and Fe(III) form blue bis-complex; further, when the pH of suspension is higher than 7, TA and Fe(III) form red tris-complex(Fig. 1a and Fig. S1). A reasonable interpretation is that the deprotonated hydroxy groups can lead to a stronger chelating ability with Fe(III). With a natural pH condition of 3.5 of the reaction system, TA and Fe(III) chelate form bis-complex. Furthermore, all three galloyl groups on the TA can form highly stable complexes with Fe(III), allowing the formation of a cross-linked TA-Fe(III) shell on PS nanospheres(Fig. 1b) (Rahim et al. 2014). To further investigate the formation mechanism of the TA-Fe(III) shell, we also coated TA on the surface of PS nanospheres without Fe(III) cross-linking. The surface of PS@TA nanospheres is rough, which means TA also can coat the surface of PS nanospheres to form a TA shell(Fig. 1c-e). It is owing to catechol-functionalized molecules and their derivatives have a high affinity for a wide variety of substrates with different surface charges (Wang et al. 2020). We also determined the zeta potential after incubating the bare PS particles with either TA or $FeCl_3$. The adsorption of TA reduced the zeta potential from − 11.0 ± 1.0 mV to − 31.8 ± 0.2 mV, whereas the value was sharply increased after incubation with $FeCl_3$ (−0.7 ± 0.3 mV). Thus, the formation of TA-Fe(III) shell can be explained by that the free TA or small TA-Fe(III) complexes initially adsorb onto the PS nanospheres surface and are subsequently cross-linked by further Fe(III) complexation. Film growth is completed when free Fe(III) in the bulk solution is consumed.

After adding TA and Fe(III) to the system, the color of the PS dispersion immediately changed from milky white to dark (Fig. 2a-b and Fig S2). The monodispersity of the colloidal building blocks has an essential influence on the assembled photonic structures and the resultant optical properties. As shown in Fig. 2c-l, it is noted that the synthesized PS@Fe(III)-TA nanospheres with a better monodispersity at a higher

temperature of 60°C. This may be due to the more intense Brownian motion at high temperatures, making it different for the nanospheres to agglomerate during the coating process. At the same temperature, the stirring time (20 s and 1 h) has no apparent effect on the color or the film thickness, which means that the film formation process is completed instantly. After ultrasonic treatment for 1 hour, it can be found that the surface of PS@Fe(III)-TA nanospheres prepared by stirring at 60°C for 20 s is still rough (Fig. S3), indicating that the Fe(III)-TA shell is relatively stable.

Chemical components analysis

XPS was used to compare and analyze the chemical compositions and surface structures of the fabric before and after treatment. As shown in Fig. 3a, the XPS spectra indicate that the original cotton fabric(CF) and PS@CF contain C and O elements. While the appearance of Fe2p peaks in the CF coated with PS@TA-Fe(III) nanoparticles indicated the integration of Fe onto the structurally colored fabric surface. Figure 3b-d shows the Cls spectrum on the surface of CF, PS@CF, and PS@TA-Fe(III)@CF, respectively. The C1s peak of original CF in Fig. 3b originates from three different peaks: C-C bond, C-O bond, and O-C = O bond. The O-C = O bond detected in the original CF may be derived from impurities on the fiber surface itself or residues from the soaping and washing process of cotton fabric before use. The peaks at 284.6, 285.5, 286.5, 289, and 291.3 eV in Fig. 3c correspond to C-C, C = C, C-OH, COOR, and $\pi \rightarrow \pi^*$ species, respectively (Zhou et al. 2018). The existence of C = C in PS@CF can be attributed to the introduction of methacrylic acid in preparing PS nanospheres. Compared with CF (C-OH), the content of hydrophilic groups (-COOH) in PS nanospheres is less, so the peak intensity and peak area of C-OH are reduced, which is consistent with previous reports. In addition, due to the dehydration and condensation of carboxylated PS nanoparticles with hydroxyl groups on the surface of cotton fibers, the peak corresponding to the formed COOR bond is 289 eV. Because TA is rich in phenolic hydroxyl groups, PS@TA-Fe(III)@CF contains more C – O (13%) than PS@CF (2.7%). Besides, the new peak at 289.5 eV is attributed to the C = O of aromatic carboxylate in TA. The fitted high-resolution O1s spectrum from PS@TA-Fe(III)@CF (Fig. 3e) provides evidence for components corresponding to Fe-O at 531.7 eV, C = O at 532.2 eV, Fe-OH at 533.4 eV, C-O at 533.5 eV (Rahim et al. 2014; Qian et al. 2020). For the valence of iron in PS@TA-Fe(III)@CF, the Fe 2p spectrum was analyzed using the method described by Mark C. Biesinger (Biesinger et al. 2011), and the presence of Fe(II) and Fe(III) was analyzed by spectral reconstruction. There are obvious peaks at about 710.3 eV (Fe(II) Fe 2p3/2), 723.9 eV (Fe(II) Fe 2p1/2) and 712.0 eV (Fe(III) Fe 2p3/2), 725.6 ev (Fe(III) Fe 2p1/2), indicating that iron exists in two valence states at the same time (Fig. 3f). The above results indicate that TA can reduce Fe(III) to Fe(II), both of which can be complexed with TA to form metal chelates, which are coated on the surface of PS nanoparticles to prepare the structurally colored fabric.

Optical properties of the structurally colored cotton fabric

The ACAs with saturated, non-iridescent, and high fastness structural color on cotton fabric were fabricated by gravity deposition self-assembly using PS@TA-Fe(III) nanospheres as the building blocks. As shown in Fig. 4a, various color fabric ranging from blue to magenta and purple could be obtained with

different sized PS. The top-view SEM image reveals that the fabricated ACAs assembled in a random close-packed structure with uneven surface and certain roughness(Fig. 4b). Moreover, the corresponding two-dimensional fast Fourier transform (2D FFT) image shown in the inset of Fig. 4b presents a discrete donut pattern, which firmly evidence the isotropic and short-range order of the resultant ACAs (Yi et al. 2017), and agreeing with the amorphous structure presented in SEM images. The amorphous arrangement of the resultant ACAs coating is probably due to the reduced surface charge of the PS@TA-Fe(III) nanospheres, which will interrupt their self-assembly process. For comparison, we employed PS nanospheres to obtain the long-range ordered PCs coatings on cotton fabric. Because of their highly charged surfaces, PS nanospheres could assemble into highly ordered 3D lattice (Fig. S4) by balancing the repulsive and attractive interactions between PS nanospheres during the solvent evaporation process. In comparison, the surface charge of the PS@TA-Fe(III) nanospheres is almost zero (−0.7 ± 0.3 mV), which suggests that the PS@TA-Fe(III) nanospheres were not sufficiently stable and may partially aggregate during the self-assembly process. In the initial stage of the colloid assembly process, the concentration of dispersion is relatively low, the distances between the PS@TA-Fe(III) nanospheres are relatively large, resulting the particles randomly move in the solution. As the solvent was gradually evaporated, the neighboring particles become closer to each other, which results in the enhanced repulsion and Van der Waals forces between colloidal particles (Li et al. 2019, 2021). However, as the surface charge of PS nanopheres was almost completely inhibited by the coating of TA-Fe(III) shell, the attractive interactions will take up dominant position. Therefore, the PS@TA-Fe(III) nanospheres tend to aggregate in a short distance in the solution, that contributed to the short-range ordered structures of ACAs. Besides, the bumpy surfaces of the PS@TA-Fe(III) nanospheres may also contribute to the formation of short-range ordered structures, rather than long-range ordered structures (Kawamura et al. 2016; Kohri 2019).

Generally, the colloidal PCs with a flat surface can increase specular reflectivity and show dazzling metallic luster (Michinari et al. 2015). However, the bumpiness and roughness of the prepared ACAs significantly reduced the specular reflection but increased the diffuse reflection of the reflected light, producing gentle and bright structural colors(Fig. 4c). The corresponding reflection spectra are shown in Fig. 4d, all prepared structurally colored fabric possesses two characteristic peaks that contribute to their structural colors. We suspect that the structural colors of PS@TA-Fe(III) coating can be attributed to two mechanisms: photonic pseudo bandgap formed by coherent scattering of ACAs with long-range disorder and short-range order, and Mie scattering resonance of nanospheres. The peaks derived from Mie scattering resonance of nanospheres are located in the ultraviolet and near-ultraviolet region, and the peaks derived from coherent scattering peaks of the structure are located in the visible region. With the increase of PS core, both of the peaks are red-shifted. When the PS cores are 180, 190 and 210 nm, Mie scattering peak of nanospheres located in ultraviolet region. According to Bragg's theory, they appear blue, cyan, and green, respectively. When the PS cores are 245nm and 280nm, the peaks derived from Mie scattering resonance red-shift to the near-ultraviolet region, and the reflection in the purple region increases, so the prepared structurally colored fabric exhibits color mixing due to the dual visible reflections.

The short-range arrangement of the ACAs provide a distinct separation between the adjacent scatterers, resulting in the formation of an isotropic photonic pseudo-band gap. From the optical images, it can be observed that the color of the structurally colored fabric (Fig. 5a) display virtually identical structural colors at different viewing angles under ambient illumination. The angle-resolved reflection spectra were measured to quantify the optical properties of the as-prepared structurally colored fabric. When the detection angle was varied from 0° to 50° relative to the light source (see the detection mode in Fig. 5b), the reflection peak position appeared at almost the same position(Fig. 5c). This indicates that the colors of the fabricated ACAs are nearly angle-independent, i.e., non-iridescent. The angle-independency might be attributed to the isotropic nature of ACAs, which has verified that the PS@TA-Fe nanospheres are arranged as ACAs on the surface of cotton fabric as discussed before.

Robustness of PS@TA-Fe(III) coatings on flexible cotton fabric and wastewater generated in the prepartion process

The robustness of the structural color coating on the fabric is crucial for its practical application. Owing to the high affinity for almost all material surfaces of TA, the force between PS@TA-Fe(III) nanospheres and between PS@TA-Fe(III) nanospheres and fabric substrate is greatly enhanced, so the structural stability of PS@TA-Fe(III) coatings can be effectively improved. To confirm the high color fastness of the coating, we investigated the damage resistance performance of PS@TA-Fe(III) coating and that of PS coating. A folding test of cotton fabric with PS@TA-Fe(III) coating is demonstrated in Fig. 6a. After 50 cycles of folding test, the structural color coating of fabric had slight cracks and abscission. Figure 6b shows the optical image of PS coating on black cotton fabric and PS@TA-Fe(III) coating on white cotton fabric before and after rubbing and simulated washing tests. After 10 cycles of sandpaper abrasion test and the 6 cycles of simulated washing test, the PS coating was worn off, and the color of the coating faded. By contrast, the cotton fabric with PS@TA-Fe(III) coating remained intact, and the color was almost retained. As shown in the corresponding SEM image, much peeling along the abrasion direction was observed on the surface of the fabric with PS coating. Moreover, after washing, the cotton surface fiber was exposed because the PS nanoparticles on the surface of the cotton massively decreased (Fig. 6c). As a result, compared to the PS coating, the PS@TA-Fe(III) coating exhibited increased resistance to bending, abrasion, and washing treatment, indicating PS@TA-Fe(III) coating has robust mechanical properties and structural stability.

The traditional dying process causes severe water pollution due to contamination from residual colorants and dying assistant, which are impossible to be naturally degraded. The recent global interest in ecological textiles and sustainable development has spurred research into the biomimetic structural coloration of textiles. In this work, we compared the wastewater produced in the dyeing process of cotton fabric with traditional reactive dyes and that produced in the preparation of PS@TA-Fe(III) nanospheres. As shown in Table 1, the wastewater from reactive dyeing is higher in BOD5, COD, chroma, and pH, and poorer in biodegradability than that from the preparation of structural dyed fabric, which does not meet the class I discharge standard(GB 4278 – 2012). However, the BOD_5, COD, BOD_5/COD value, chromaticity and pH value of the wastewater generated during the preparation of PS@TA-Fe(III) nanospheres all meet

the discharge standard, which proves that the preparation process of this method is environmentally friendly and the prepared structural colored cotton fabric is green and healthful.

Conclusions

In conclusion, monodispersed PS@TA-Fe(III) nanospheres with intense light absorption and interface adhesion were synthesized for non-iridescent structural coloration of textiles. Through the self-assembly process, PS@TA-Fe(III) ACAs with short-range ordered structures were created because of the scattering light absorbing ability of TA-Fe(III) shell and the weak repulsion interactions between PS@TA-Fe(III) nanospheres. The ACAs show non-iridescent property with high color contrast, and their reflection color could be adjusted by varying the size of the PS core material. Besides, prepared structurally colored cotton fabric shows strong structural stability after folding, sandpaper abrasion, and simulated washing tests. This facile and inexpensive fabrication strategy can provide a novel method to design and fabricate bright and non-iridescent structural colored materials, which may have promising applications in the future.

Declarations

Ethics approval and consent to participate

No human or animals are involved in our experiments so it is not applicable.

Consent for publication

All co-authors have approved the manuscript for publication.

Availability of data and materials

The authors confirm that all the data and materials are available.

Acknowledgments Tieling Xing acknowledge the support from the National Natural Science Foundation of China(51973144, 51741301) and the Foundation of Jiangsu Engineering Research Center of Textile Dyeing and Printing for Energy Conservation, Discharge Reduction and Cleaner Production(Q811580621). Xiaowei Zhu is grateful for the financial support from the Postgraduate Research & Practice Innovation Program of Jiangsu Province (No. KYCX21-2960). Tianchen Wei thanks the support from the National Undergraduate Training Program for Innovation and Entrepreneurship, China (202010285045, 202010285036Z), and Yichen Li thanks the support from the China Postdoctoral Science Foundation (2022M712302).

Authors contribution Xiaowei Zhu: Conceptualization, Methodology, Investigation, Writing - original draft, Visualization. Tianchen Wei: Data curation, Instrument appointment and testing. Yijiang Li: Investigation, Data curation. Yichen Li: Data curation, Writing - review & editing, Supervision Tieling Xing:

Conceptualization, Methodology, Writing - review & editing, Supervision, Project administration. Matthew D. Shawkey and Guoqiang Chen: Supervision, Writing - review & editing.

Funding This work was financially supported bythe National Natural Science Foundation of China (51973144, 51741301); Postgraduate Research & Practice Innovation Program of Jiangsu Province (No. KYCX21-2960); the National Undergraduate Training Program for Innovation and Entrepreneurship, China (202010285045, 202010285036Z); the Foundation of Jiangsu Engineering Research Center of Textile Dyeing and Printing for Energy Conservation, Discharge Reduction and Cleaner Production(Q811580621); and the China Postdoctoral Science Foundation (2022M712302).

Confict of interest The authors declare that they have no known competing financial interests or personal relationships that could have appeared to influence the work reported in this paper.

References

1. Biesinger MC, Payne BP, Grosvenor AP, et al (2011) Resolving surface chemical states in XPS analysis of first row transition metals, oxides and hydroxides: Cr, Mn, Fe, Co and Ni. Appl Surf Sci 257(7): 2717–2730. https://doi.org/10.1016/j.apsusc.2010.10.051
2. Chen GW, Yi B, Huang YY, et al (2019) Development of bright and low angle dependence structural colors from order-disorder hierarchical photonic structure. Dyes Pigm 161: 464–469. https://doi.org/10.1016/j.dyepig.2018.09.039
3. Ejima H, Richardson JJ, Liang K et al (2013) One-step assembly of coordination complexes for versatile film and particle engineering. Science 341: 154–157. https://doi.org/10.1126/science.1237265
4. Ge DT, Yang LL, Wu GX, Yang S (2014) Angle-independent colours from spray coated quasi amorphous arrays of nanoparticles: Combination of constructive interference and Rayleigh scattering. J Mater Chem C 2(22): 4395. https://doi.org/10.1039/C4TC00063C
5. Guo JL, Yuan P, Hirotaka E, et al (2014) Engineering multifunctional capsules through the assembly of metal–phenolic networks. Angew Chem Int Ed Engl 53: 5546–5551. https://doi.org/10.1002/anie.201311136
6. Iwata M, Teshima M, Seki T, et al (2017) Bio-inspired bright structurally colored colloidal amorphous array enhanced by controlling thickness and black background. Adv Mater 29 (26): 1605050. https://doi.org/10.1002/adma.201605050
7. Kawamura A, Kohri M, Morimoto G, et al (2016) Full-color biomimetic photonic materials with iridescent and non-iridescent structural colors. Sci Rep 6: 33984. https://doi.org/10.1038/srep33984
8. Kohri M, Nannichi Y, Taniguchi T, Kishikawa K (2015) Biomimetic non-iridescent structural color materials from polydopamine black particles that mimic melanin granules. J Mater Chem C 3(4): 720–724. https://doi.org/10.1039/c4tc02383h

9. Kohri M (2019) Artificial melanin particles: new building blocks for biomimetic structural coloration. Polymer J 51(11): 1127–1135. https://doi.org/10.1038/s41428-019-0231-2
10. Kohri M (2020) Progress in polydopamine-based melanin mimetic materials for structural color generation. Sci Technol Adv Mat 21(1): 833–848. https://doi.org/10.1080/14686996.2020.1852057
11. Li YC, Wang XH, Hu MA, et al (2019) Patterned SiO_2/Polyurethane acrylate inverse opal photonic crystals with high color saturation and tough mechanical strength. Langmuir 35(44): 14282–14290. https://doi.org/10.1021/acs.langmuir.9b02485
12. Li YC, Fan QS, Wang XH, et al (2020) Shear-induced assembly of liquid colloidal crystals for large-scale structural coloration of textiles. Adv Funct Mater 31: 2010746. https://doi.org/10.1002/adfm.202010746
13. Liu PM, Chen JL, Zhang ZX, et al (2018) Bio-inspired robust non-iridescent structural color with self-adhesive amorphous colloidal particle arrays. Nanoscale 10: 3673–3679. https://doi.org/10.1039/C7NR08056E
14. Liu PM, Liu XJ, Ji MH, et al (2020) A highly colorimetric photonic film composed of non-close-packed melanin-like colloidal arrays. J Colloid Interf Sci 580: 573–582. https://doi.org/10.1016/j.jcis.2020.07.067
15. Meng Y, Tang BT, Ju BZ, et al (2017) Multiple colors output on voile through 3D colloidal crystals with robust mechanical properties. ACS Appl. Mater. Inter. 9: 3024–3029. https://doi.org/10.1021/acsami.6b14819
16. Michinari K, Yuri N, Tatsuo T, Keiki K (2015) Biomimetic non-iridescent structural color materials from polydopamine black particles that mimic melanin granules. J Mater Chem C 3: 720–724. https://doi.org/10.1039/c4tc02383h
17. Okada T, Hosoyamada S, Takada C, Ohta C (2021) Monodisperse clay microballs for tuning the pseudogaps by adsorption in amorphous photonic structures. Chemphotochem 5: 32–35. https://doi.org/10.1002/cptc.202000160
18. Perron NR, Brumaghim JL (2009) A review of the antioxidant mechanisms of polyphenol compounds related to iron binding. Cell Biochem Biophys 53(2): 75–100. https://doi.org/10.1007/s12013-009-9043-x
19. Qian YH, Chen SQ, He C et al (2020) Green fabrication of tannic acid-inspired magnetic composite nanoparticles toward cationic dye capture and selective degradation. ACS Omega 5: 6566–6575. https://dx.doi.org/10.1021/acsomega.9b04304
20. Rahim MA, Ejima H, Cho KL, et al (2014) Coordination-driven multistep assembly of metal–polyphenol films and capsules. Chem Mater 26: 1645–1653. https://doi.org/10.1021/cm403903m
21. Shen H, Liang Q, Song L, et al (2020) Facile fabrication of mechanically stable non-iridescent structural color coatings. J Mater Sci 2020; 55: 2353–2364. https://doi.org/10.1007/s10853-019-04118-y
22. Shi XD, He JL, Xie XL, et al (2019) Photonic crystals with vivid structure color and robust mechanical strength. Dyes Pigm 137–143. https://doi.org/10.1016/j.dyepig.2019.02.023

23. Shi XD, He JL, Wu LC, et al (2020) Rapid fabrication of robust and bright colloidal amorphous arrays on textiles. J Coat Technol Res 2020; 17 (4): 1033–1042. https://doi.org/10.1007/s11998-019-00311-5
24. Sileika TS, Barrett DG, Zhang R, et al (2013) Colorless multifunctional coatings inspired by polyphenols found in tea, chocolate, and wine. Angew. Chem. Int. Ed. 2013; 52: 10766–10770. https://doi.org/10.1002/ange.201304922
25. Takeoka Y (2012) Angle-independent structural coloured amorphous arrays. J Mater Chem C 22(44): 23299. https://doi.org/10.1039/C2JM33643J
26. Takeoka Y, Yoshioka S, Takano A, et al (2013) Production of colored pigments with amorphous arrays of black and white colloidal particles. Angew Chem 125 (28): 7402–7406. https://doi.org/10.1002/ange.201301321
27. Wang RX, Zhao XT, Lan YY, et al (2020) In situ metal-polyphenol interfacial assembly tailored superwetting PES/SPES/MPN membranes for oil-in-water emulsion separation. J Membrance Sci 615: 118566 https://doi.org/10.1016/j.memsci.2020.118566
28. Wang YQ, Chen S, Zhao SY, et al (2020) Interfacial coordination assembly of tannic acid with metal ions on three-dimensional nickel hydroxide nanowalls for efficient water splitting. J Mater Chem A 8: 15845–15852. https://doi.org/10.1039/D0TA02229B
29. Xiao M, Li YW, Allen MC, et al (2015) Bio-inspired structural colors produced via self-assembly of synthetic melanin nanoparticles. ACS Nano 9: 5454. https://doi.org/10.1021/acsnano.5b01298
30. Xiao M, Hu Z, Wang Z, et al (2017) Bioinspired bright noniridescent photonic melanin supraballs. Sci Adv 3: e1701151. https://doi.org/10.1126/sciadv.1701151
31. Xiao M, Shawkey MD, Dhinojwala A (2020) Bioinspired melanin-based optically active materials. Adv Optical Mater 8(19): 2000932. https://doi.org/10.1002/adom.202000932
32. Yang X, Ge D, Wu G, et al (2016) Production of structural colors with high contrast and wide viewing angles from assemblies of Polypyrrole black coated Polystyrene nanoparticles. ACS Appl Mater Interfaces 8(25): 16289–16295. https://doi.org/10.1021/acsami.6b03739
33. Yang DP, Hu YWT, Hu Y, Huang SM (2020) Two birds with one stone: manipulating colloids assembled into amorphous and ordered photonic crystals and their combinations for coding – decoding. J Phys Chem C 124: 6328–6336. https://doi.org/10.1021/acs.jpcc.0c00344
34. Yi B, Shen HF (2017) Facile fabrication of crack-free photonic crystals with enhanced color contrast and low angle dependence. J Mater Chem C 5: 8194–820. https://doi.org/10.1039/C7TC01549F
35. Yuan W, Zhou N, Shi L, Zhang KQ (2015) Structural coloration of colloidal fiber by photonic band gap and resonant Mie scattering. ACS Appl Mater Interfaces 7(25): 14064–14071. https://doi.org/10.1021/acsami.5b03289
36. Zhang Y, Han P, Zhou H, et al (2018) Highly brilliant noniridescent structural colors enabled by graphene nanosheets containing graphene quantum dots. Adv Funct Mater 28: 1802585. https://doi.org/10.1002/adfm.201802585

37. Zhou L, Li YC, Liu GJ, et al (2016) Study on the correlations between the structural colors of photonic crystals and the base colors of textile fabric substrates. Dyes Pigm 133: 435–444. https://doi.org/10.1016/j.dyepig.2016.06.032
38. Zhou QQ, Chen GQ, Xing TL (2018) Facile construction of robust superhydrophobic tea polyphenol/Fe@cotton fabric for self-cleaning and efficient oil–water separation. Cellulose 25: 1513–1525. https://doi.org/10.1007/s10570-018-1654-1
39. Zhu XW, Wei TC, Mia MS, et al (2021) Preparation of PS@PDA amorphous photonic structural colored fabric with vivid color and robust mechanical properties based on rapid polymerization of dopamine. Colloid Surface A 622: 126651. https://doi.org/10.1016/j.colsurfa.2021.126651

Tables

Table 1 is available in the Supplemental Files section.

Figures

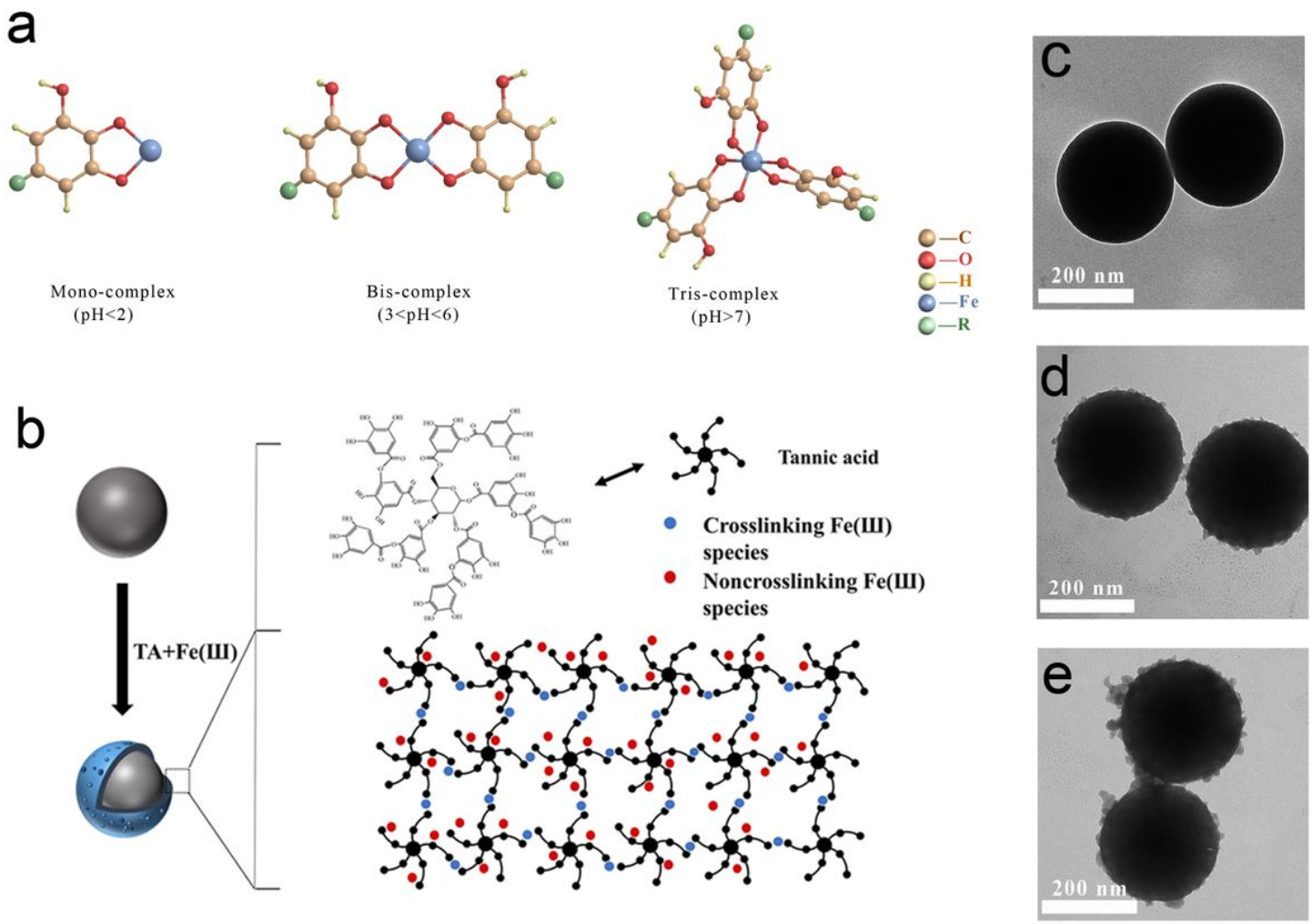

Figure 1

(a) pH-dependent formation of dominant TA-Fe(III) complexation state, R represents the remainder of the TA molecule; (b) Schematic of the fabrication of PS@TA-Fe(III); the TEM images of (c) PS nanospheres(NPs),(d) PS@TA NPs

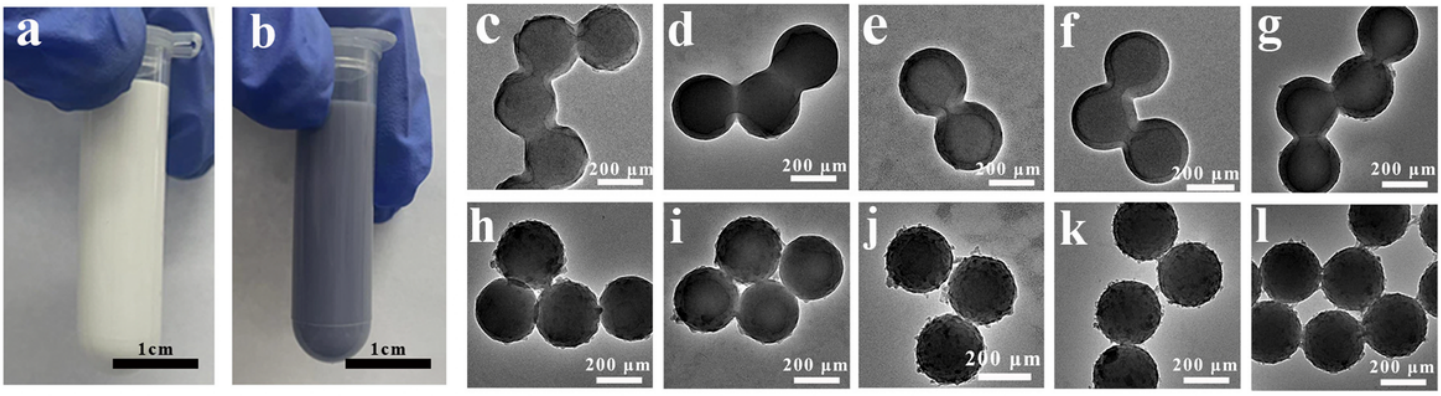

Figure 2

Photograph of (a) PS and (b) PS@Fe(III)-TA NPs dispersion (≈0.2wt%); (c-l) TEM images of PS NPs after Fe(III)-TA coating with different reaction conditions (the reaction time from left to right is 20s, 5min, 10min, 30min, 1h; the reaction temperature in the upper row is 25°C, the lower row is 60°C)

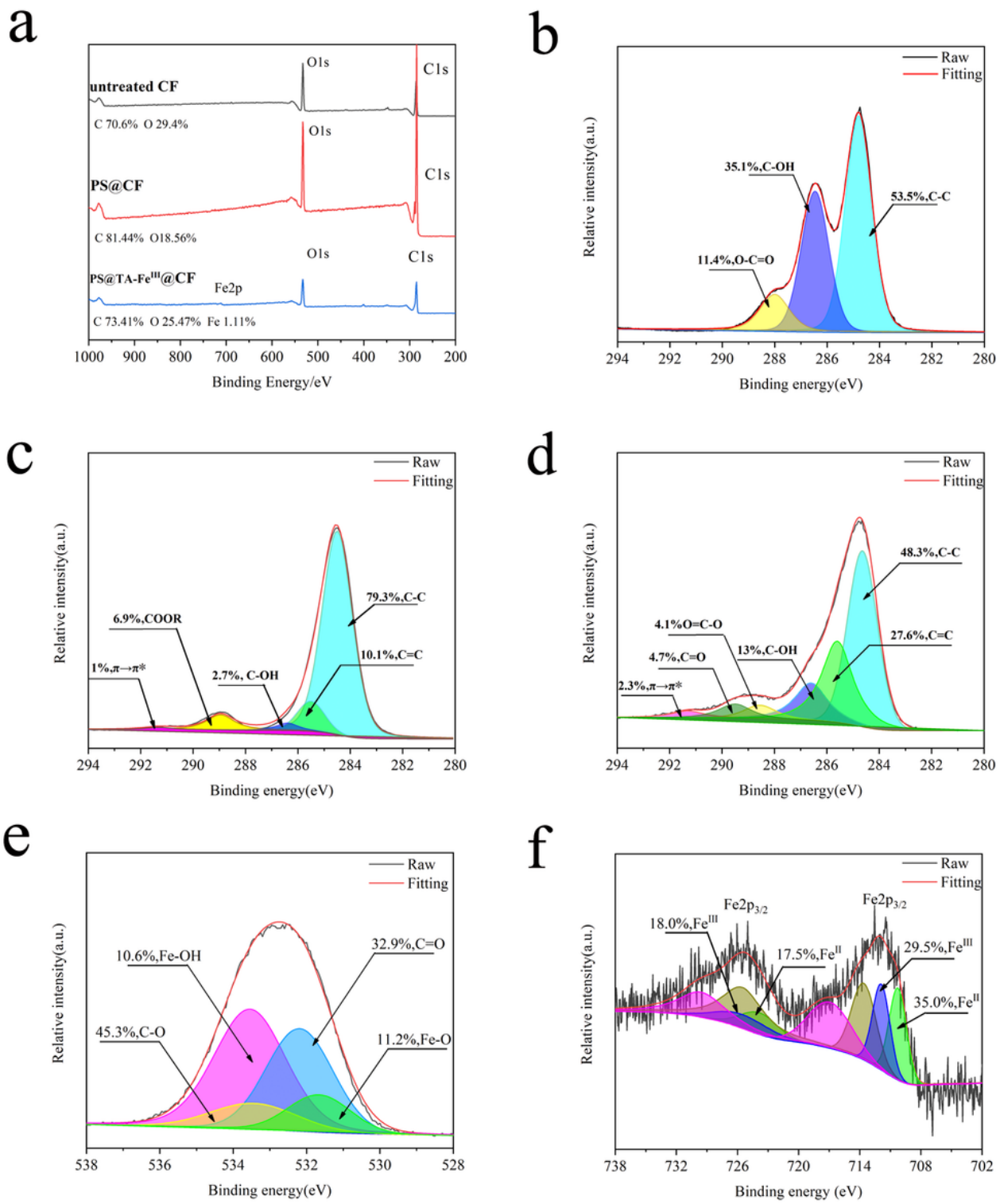

Figure 3

(a) XPS survey spectra of the untreated CF, PS_{180}@CF, and PS_{180}@TA-Fe(III)@CF; high resolution XPS spectrum of C1s of (b) untreated CF, (c) PS_{180}@CF, (d) PS_{180}@TA-Fe(III)@CF; high resolution XPS spectrum of (e) O1s and (f) Fe 2p of P PS_{180}@TA-Fe(III)@CF

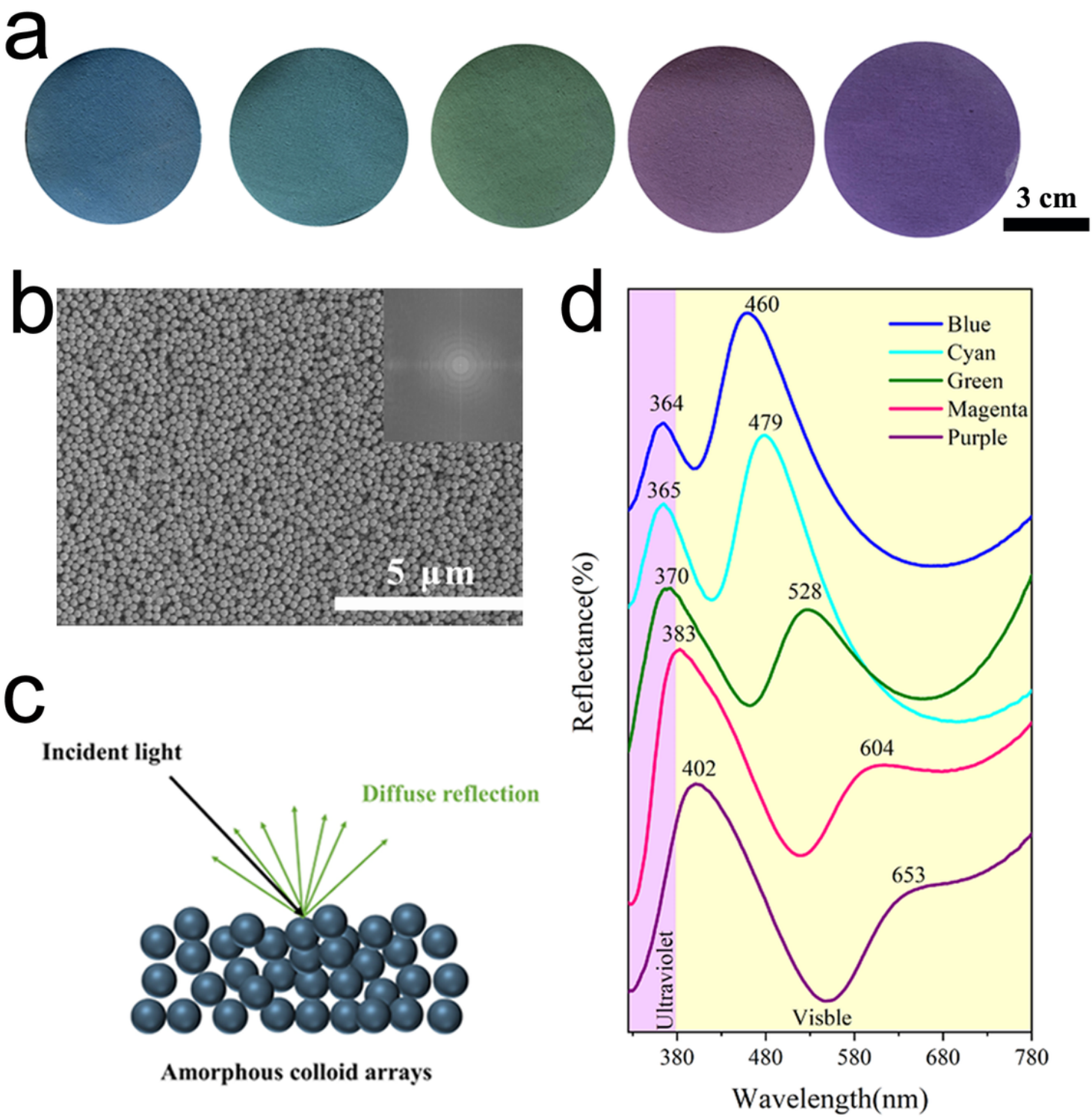

Figure 4

(a) Photographs of the structurally colored cotton fabric coated with PS@TA-Fe(III) NPs; (b) SEM images of the structurally colored cotton fabric formed by PS@TA-Fe(III) NPs (the diameters of PS cores are 180 nm) and the inset is corresponding 2D FFT of (b); (c) the schematic of light reflection on amorphous colloidal arrays surface and (d) Reflection spectra of various structurally colored cotton fabric fabricated

by PS@TA-Fe(III) NPS; the diameters of PS cores are 180 nm (blue), 190 nm (cyan), 210 nm (green), 245 nm (magenta) and 280 nm (purple)

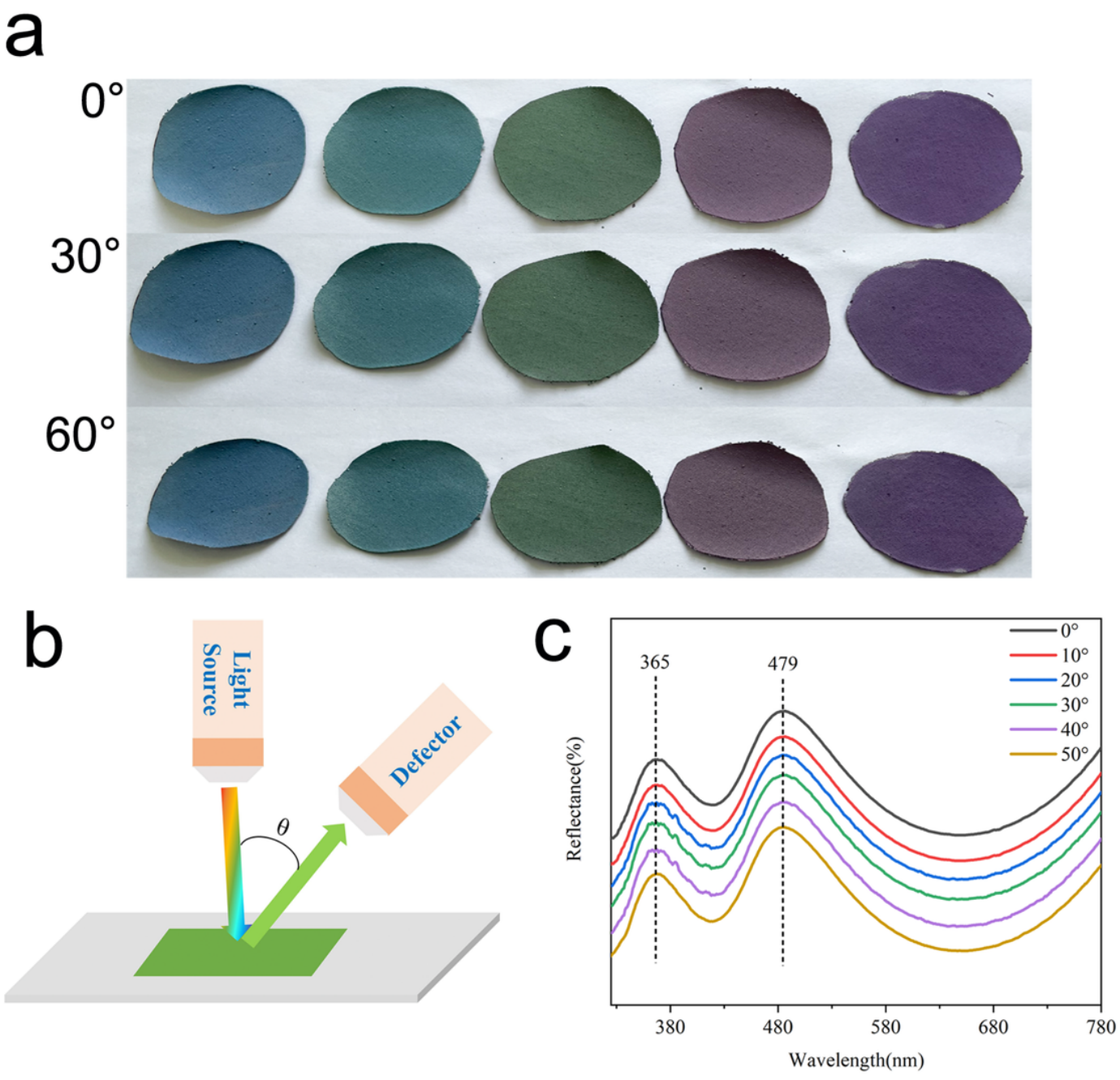

Figure 5

(a) Digital photo images of structurally colored cotton fabric at different viewing angles; (b) Reflection spectra of the blue structurally colored cotton fabric with different incident angles; (c) Plots of peak

wavelengths for the reflection spectra as a function of incident angle

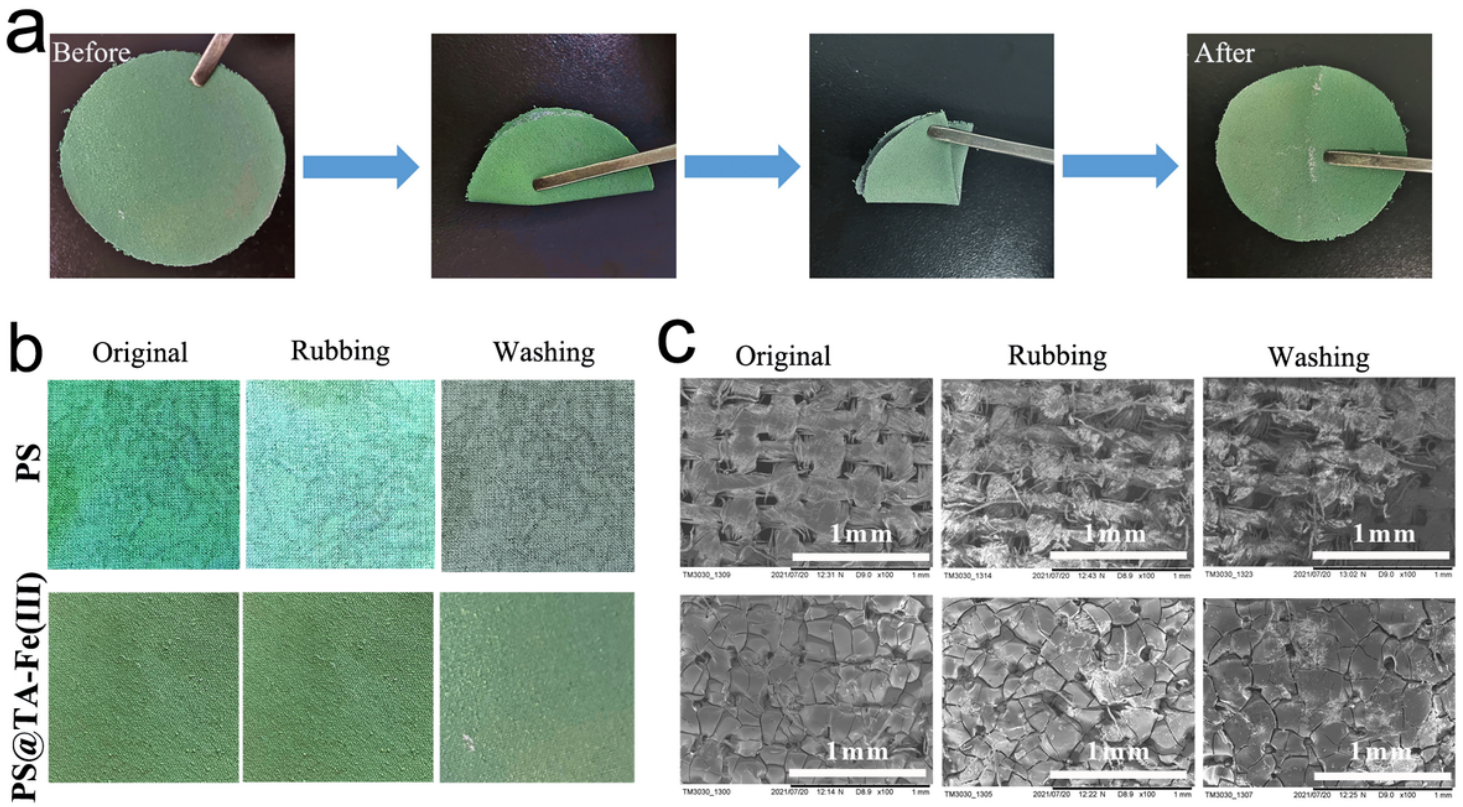

Figure 6

(a) Folding test of the cotton fabric of PS@TA-Fe(III) coatings; (b) optical images of PS and PS@TA-Fe(III) coating on cotton fabric before and after rubbing and simulated washing tests and (c) the corresponding SEM images under different magnification.

Supplementary Files

This is a list of supplementary files associated with this preprint. Click to download.

- SupportinginformationR1.doc
- floatimage1.png
- Table1Thewaterqualityofdyeingwastewater.docx